Anisotropic phase transition in the asymmetric three-states clock model

1986 J. Phys. A: Math. Gen. 19 1957

(http://iopscience.iop.org/0305-4470/19/10/036)

J. Phys. A: Math. Gen. 19 (1986) 1957-1966. Printed in Great Britain

Anisotropic phase transition in the asymmetric three-states clock model

T Vescan, V Rittenberg and G von Gehlen

Physikalisches Institut der Universität Bonn, Nussallee 12, D-5300 Bonn 1, West Germany

Received 5 September 1985

Abstract. The three-states asymmetric clock model is considered in the x-continuum limit. Along the x axis the interaction has the Potts symmetry and the Hamiltonian thus obtained is non-Hermitian.

Using finite-size scaling one obtains only one phase transition, which is anisotropic, between a low-temperature ferromagnetic phase and a high-temperature modulated phase. Estimates for some critical exponents are given.

1. Introduction

The phase structure of the two-dimensional three-states asymmetric clock model (Ostlund 1981, Huse 1981) remains a controversial issue (see Duxbury *et al* 1984 and references therein). The system is defined by a partition function Z and an action S as follows

$$Z = \sum_{(\alpha)} \exp(-S) \tag{1.1}$$

$$S = -\sum_{x,\tau} \{g_x \cos[\tfrac{2}{3}\pi(\alpha_{x+1,\tau} - \alpha_{x,\tau})] + g_\tau \cos[\tfrac{2}{3}\pi(\alpha_{x,\tau+1} - \alpha_{x,\tau}) - \varphi]\} \tag{1.2}$$

where $\alpha_{x,\tau} = 0, 1, 2$, and $0 \leqslant \varphi \leqslant \frac{1}{3}\pi$. For $g_x = g_\tau \sim 1/T$ one probably has a phase diagram with the general structure shown in figure 1. However, the details are controversial.

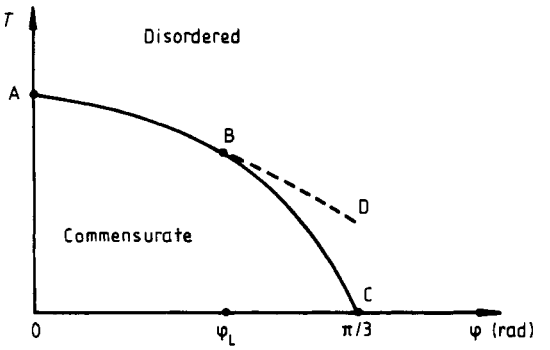

Figure 1. Phase diagram for the chiral three-states clock model (the points A, B, C and D are explained in the text). φ_L is the value of the asymmetry angle corresponding to the Lifshitz point.

0305-4470/86/101957+10$02.50

One distinguishes a low-temperature commensurate phase separated by the curve AB from a disordered phase through a Potts transition according to Howes (1982) or a chiral transition (Huse and Fisher 1982, Duxbury *et al* 1984). The Lifshitz point B corresponds to an angle φ_L and the curves BC and BD are the borders of the incommensurate phase (Selke and Yeomans 1982). Now the very existence of the Lifshitz point at a non-zero angle φ is questioned (Haldane *et al* 1983, Schulz 1983, von Gehlen and Rittenberg 1984).

The understanding of the phase diagram is obscured by convergence problems so that different authors using different approaches have reached contradictory conclusions. Clearly, in order to clarify the situation as many different methods as possible should be applied.

Let us concentrate here on the application of finite-size scaling (FSS) methods (Nightingale 1982) to our system (1.2). Since the action is asymmetric with respect to the x and τ directions, FSS may be applied either

(1) to strips finite in the τ direction (which is the direction where incommensurate structures are expected to show up). This has been studied by von Gehlen and Rittenberg (1984) in the τ continuum limit

$$g_\tau \to 0 \qquad g_x \to \infty \qquad 1/T = g_\tau \exp(\tfrac{3}{2} g_x) \qquad \text{fixed} \tag{1.3}$$

(we shall summarise the main results later)

(2) or to strips finite in the x direction (which has the Potts symmetry). This has been investigated recently by Duxbury *et al* (1984) for the symmetric situation $g_x = g_\tau$.

The purpose of the present paper is to present a detailed study of the anisotropic limit

$$g_x \to 0 \qquad g_\tau \to \infty \qquad 1/T = g_x \exp(\tfrac{3}{2} g_\tau) \qquad \text{fixed} \tag{1.4}$$

of the transfer matrix for case 2. Since we find very good convergence of the FSS extrapolation in this limit, a clear picture of a single asymmetric phase transition will emerge.

Before proceeding to present our calculations, we shall first review a few details relevant to the understanding of our work.

In the limit (1.3) the transfer matrix of the action (1.2) leads (after a duality transformation) to the Hamiltonian of a one-dimensional quantum chain:

$$\bar{H}^D = \sum_{k=1}^{N} (2\cos\varphi - e^{i\varphi}\sigma_k - e^{-i\varphi}\sigma_k^+) - T \sum_{k=1}^{N} (\Gamma_k \Gamma_{k+1}^+ + \Gamma_k^+ \Gamma_{k+1}) \tag{1.5}$$

where

$$\sigma_k = \begin{pmatrix} 1 & 0 & 0 \\ 0 & \omega & 0 \\ 0 & 0 & \omega^2 \end{pmatrix}_k \qquad \Gamma_k = \begin{pmatrix} 0 & 1 & 0 \\ 0 & 0 & 1 \\ 1 & 0 & 0 \end{pmatrix}_k \tag{1.6}$$

and $\omega = \exp(\frac{2}{3}\pi i)$. In (1.5) k labels the sites of the chain of lengths N.

Von Gehlen and Rittenberg (1984) have determined the boundary of the commensurate phase (ABC in figure 1). The wavevector K was obtained from the spacing of the zeros of the energy gap of the Hamiltonian (1.5) according to the methods of Hoeger *et al* (1985). The result for the critical exponents of the correlation length ξ

and K is

$$1/\xi = |T - T_c|^{\nu_x} \qquad K = |T - T_c|^{\nu_{\tau_1}} \tag{1.7}$$

with

$$\nu_x \approx 1 \qquad \nu_{\tau_1} \approx 0.5 \tag{1.8}$$

for all values of φ down to $\varphi \approx \pi/10$. For small values of φ the convergence gets poorer. However, the pattern of the zeros of the energy gap is smooth and follows a scaling law, so that no room seems to be left for a Lifshitz point B at a non-zero value of φ. More details are contained in von Gehlen and Rittenberg (1986).

In case 2 above, the transfer matrix is non-Hermitian. Duxbury *et al* (1984) have calculated the lowest eigenvalues λ_0 and λ_1 of this transfer matrix and obtain

$$\xi_\tau^{-1} = \ln\left(\frac{\lambda_0}{|\lambda_1|}\right) \qquad K = \tan^{-1}\left(\frac{\operatorname{Im}\lambda_1}{\operatorname{Re}\lambda_1}\right) \tag{1.9}$$

with

$$\xi_\tau^{-1} = |T - T_c|^{\nu_{\tau_2}} \qquad K = |T - T_c|^{\nu_{\tau_1}} \tag{1.10}$$

where ξ_τ is the correlation length in the τ direction. Let us furthermore define

$$\theta_1 = \nu_{\tau_1}/\nu_x \qquad \theta_2 = \nu_{\tau_2}/\nu_x. \tag{1.11}$$

Using FSS, the method of Domany and Schaub (1984) for anisotropic scaling and their own 'diagnosis' of the data, Duxbury *et al* (1984) have concluded that on the line AB on figure 1, $\theta_1 = \theta_2 = 1$, $\nu_x \approx 0.8$ compatible with a chiral transition, there is a Lifshitz point at $\varphi_L \approx \pi/4$ and for $\varphi > \varphi_L$ they get $\theta_1 < 1$ compatible with (1.5).

The anisotropic limit (1.4) of the non-Hermitian transfer matrix used by Duxbury *et al* leads to the non-Hermitian Hamiltonian

$$H = -\sum_{k=1}^{N} \sigma_k - \frac{1}{T}\sum_{k=1}^{N} (\Gamma_k \Gamma_{k+1}^{+} + \Gamma_k^{+}\Gamma_{k+1}) \tag{1.12}$$

and its dual

$$H^D = -\sum_{k=1}^{N} (\sigma_k + \sigma_k^{+}) - T\sum_{k=1}^{N} \Gamma_k \Gamma_{k+1}^{+}. \tag{1.13}$$

Notice that the φ dependence is lost in this limit, for all $\varphi \neq 0$ one obtains the same Hamiltonian. The limits (1.4) and $\varphi \to 0$ do not commute.

In § 2 we shall give a detailed study of the FSS properties of the Hamiltonians (1.12) and (1.13). A clear picture of the phase structure of H and H^D will emerge. Critical exponents and the asymmetrics (1.11) will be determined. Section 3 presents our conclusions.

2. Finite-size scaling properties

Although this should be done, we have not performed the high- and low-temperature expansions for the Hamiltonians (1.12) and (1.13) and have considered only their

finite-size scaling properties. Notice that the Hamiltonians (1.12) and (1.13) commute with the charge operator

$$Q = \sum_{k=1}^{N} q_k \qquad (\text{mod } 3) \tag{2.1}$$

where

$$q_k = \begin{pmatrix} 0 & 0 & 0 \\ 0 & 1 & 0 \\ 0 & 0 & 2 \end{pmatrix}_k . \tag{2.2}$$

The adjoints of the operators H and H^{D}, H^{+} and H^{D+}, have the property that the charge sectors 1 and 2 are interchanged. For convenience we will write

$$\lambda = 1/T \tag{2.3}$$

and denote by

$$W_n^{(Q)}(N, \lambda) = E_n^{(Q)}(N, \lambda) + \mathrm{i} F_n^{(Q)}(N, \lambda) \tag{2.4}$$

the eigenvalues of the Hamiltonians with N sites and periodic boundary conditions. Q indicates the charge sector ($Q = 0, 1, 2$) and n labels the levels: $n = 0, 1, 2, \ldots$ with

$$E_n^{(Q)}(N, \lambda) < E_{n+1}^{(Q)}(N, \lambda). \tag{2.5}$$

Obviously

$$W_n^{(1)}(N, \lambda) = W_n^{(2)*}(N, \lambda). \tag{2.6}$$

We have determined the inverse of the spin-spin correlation:

$$E(N, \lambda) = E_0^{(1)}(N, \lambda) - E_0^{(0)}(N, \lambda) \tag{2.7}$$

the wavevector

$$F(N, \lambda) = F_0^{(1)}(N, \lambda) \tag{2.8}$$

and the inverse of the energy-energy correlation

$$G(N, \lambda) = E_1^{(0)}(N, \lambda) - E_0^{(0)}(N, \lambda). \tag{2.9}$$

Finite-size scaling teaches us that one should obtain

$$\begin{aligned} E(N, \lambda) &= N^{-\theta_2} \mathscr{E}(z) \\ F(N, \lambda) &= N^{-\theta_1} \mathscr{F}(z) \\ G(N, \lambda) &= N^{-\theta_3} \mathscr{G}(z) \end{aligned} \tag{2.10}$$

where

$$z = N^{1/\nu_x}(\lambda - \lambda_c) \qquad \theta_i = \nu_{\tau_i}/\nu_x. \tag{2.11}$$

In order to obtain the critical exponents θ_i and ν_x we have constructed the functions (Kinzel 1983, Domany and Schaub 1984):

$$Y_E(N, \lambda) = \frac{\ln(E(N+1, \lambda)/E(N, \lambda))}{\ln(N/(N+1))} \tag{2.12}$$

$$Z_E(N, \lambda) = \ln\left[\frac{\mathrm{d}E(N+1, \lambda)}{\mathrm{d}\lambda}\left(\frac{\mathrm{d}E(N, \lambda)}{\mathrm{d}\lambda}\right)^{-1}\right]\left[\ln\left(\frac{N+1}{N}\right)\right]^{-1} \tag{2.13}$$

and similar expressions with $F(N, \lambda)$ and $G(N, \lambda)$ instead of $E(N, \lambda)$, i.e. $Y_F(N, \lambda)$,

$Z_F(N, \lambda)$, etc. From the equations

$$Y(N+1, \lambda_{c,N}) = Y(N, \lambda_{c,N}) = \theta_{i,N} \tag{2.14}$$

$$\tfrac{1}{2}[Z(N+1, \lambda_{c,N}) + Z(N, \lambda_{c,N})] + \theta_{i,N} = \nu_{x,N} \tag{2.15}$$

one gets approximants for the critical temperature $\lambda_c = (T_c)^{-1}$ and the critical exponents θ_i and ν_x.

Finally we have considered the 'specific heat'

$$C(N, \lambda) = -\frac{1}{N}\frac{d^2 E_0^{(0)}(N, \lambda)}{d\lambda^2} = N^{\alpha/\nu_x}\mathscr{C}(z) \tag{2.16}$$

which allows us to determine α.

We first study the Hamiltonian H (see (1.12)). In figure 2 we show the curves $Y_E(N, \lambda)$ and $Y_F(N, \lambda)$. We do so because Duxbury *et al* (1984) have noticed for $\varphi > \pi/4$ a wiggle in the function $Y_E(N, \lambda)$ and their functions $Y_E(N, \lambda)$ and $Y_F(N, \lambda)$ intersect in different places. Their functions $Y_F(N, \lambda)$ intersect at a lower temperature (the commensurate-incommensurate phase transition) and the functions $Y_E(N, \lambda)$ at a higher temperature (the incommensurate-disordered transition). As one can see from figure 2, in our case the functions $Y_E(N, \lambda)$ and $Y_F(N, \lambda)$ intersect at the same temperature indicating only *one phase transition.* (We are interested only in positive Y_E and Y_F according to (2.14).) In table 1 we give the values of $\lambda_{c,N}$, $\theta_{2,N}$ and $\nu_{x,N}$ obtained using (2.14) and (2.15) for $Y_E(N, \lambda)$ and $Z_E(N, \lambda)$. In table 2 we show the corresponding quantities obtained from $Y_F(N, \lambda)$ and $Z_F(N, \lambda)$. The estimates for λ_c, θ_i and ν_x were obtained using Vanden Broeck-Schwartz (1979) approximants as well as power fits. Similar estimates are given for H^D (see (1.13)) in table 3. In this case we have used only $Y_E(N, \lambda)$ and $Z_E(N, \lambda)$ since the imaginary part of the first excited state is small.

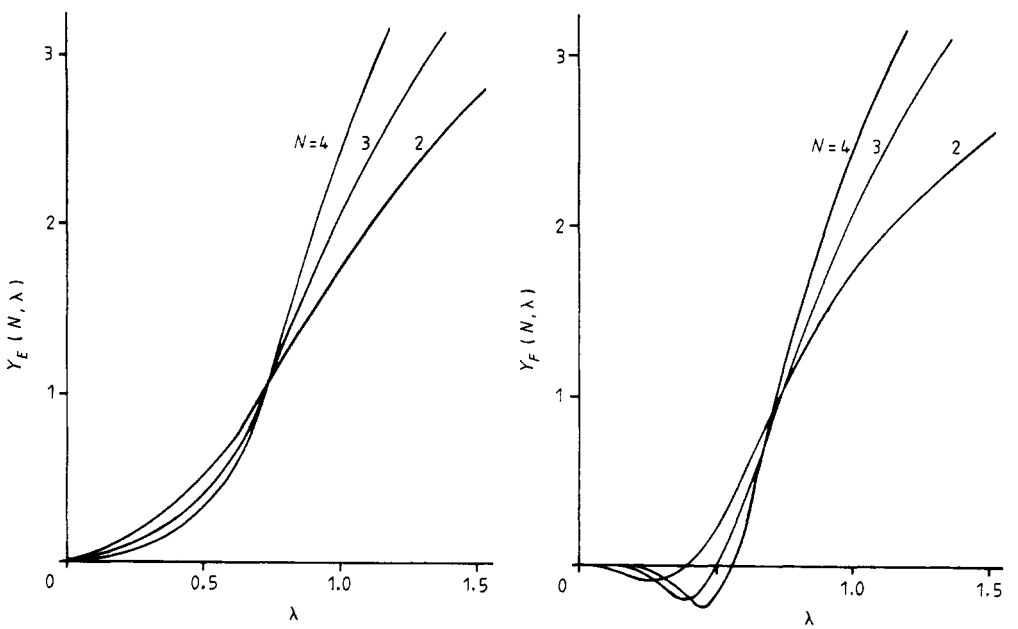

Figure 2. $Y_E(N, \lambda)$ and $Y_F(N, \lambda)$ as functions of λ, for $N = 2, 3, 4$.

Table 1. The approximants $\lambda_{c,N}$, $\theta_{2,N}$ and $\nu_{x,N}$ obtained using (2.14), (2.15) and the functions $Y_E(N,\lambda)$ and $Z_E(N,\lambda)$ for the Hamiltonian H.

Intersections $(N-1)/N/(N+1)$	$\lambda_{c,N}$	$\theta_{2,N}$	$\nu_{x,N}$
2/3/4	0.741 048 2404	1.082 67	0.633 46
3/4/5	0.708 517 0461	0.959 85	0.734 53
4/5/6	0.696 541 9038	0.901 79	0.790 27
5/6/7	0.690 618 4803	0.866 88	0.826 33
6/7/8	0.687 160 0210	0.842 94	0.851 77
7/8/9	0.684 914 7815	0.825 10	0.870 88
Estimates	0.678 ± 0.003	0.75 ± 0.03	0.95 ± 0.02

Table 2. The approximants $\lambda_{c,N}$, $\theta_{1,N}$ and $\nu_{x,N}$ obtained using (2.14), (2.15) and the functions $Y_F(N,\lambda)$ and $Z_F(N,\lambda)$ for the Hamiltonian H.

Intersections $(N-1)/N/(N+1)$	$\lambda_{c,N}$	$\theta_{1,N}$	$\nu_{x,N}$
2/3/4	0.721 940 6115	0.941 26	0.622 737
3/4/5	0.697 647 6441	0.826 93	0.710 984
4/5/6	0.688 831 7569	0.771 64	0.758 145
5/6/7	0.684 537 0343	0.737 98	0.788 441
6/7/8	0.682 077 8811	0.714 86	0.809 94
7/8/9	0.680 517 1658	0.697 73	0.826 20
Estimates	0.676 ± 0.002	0.64 ± 0.02	0.90 ± 0.04

Table 3. The approximants $\lambda_{c,N}$, $\theta_{2,N}$ and $\nu_{x,N}$ obtained using (2.14), (2.15) and the functions $Y_E(N,\lambda)$ and $Z_E(N,\lambda)$ for the Hamiltonian H^D.

Intersections $(N-1)/N/(N+1)$	$\lambda_{c,N}$	$\theta_{2,N}$	$\nu_{x,N}$
2/3/4	0.608 237 1911	0.922 979	0.658 19
3/4/5	0.635 513 1663	0.813 810	0.775 14
4/5/6	0.647 095 1939	0.760 058	0.843 93
5/6/7	0.653 425 5329	0.726 382	0.891 27
6/7/8	0.657 421 3556	0.702 438	0.926 73
Estimates	0.668 ± 0.007	0.64 ± 0.02	1.03 ± 0.02

From tables 1-3 and figure 2 we conclude that one has only *one phase transition* with

$$\lambda_c = 0.675 \pm 0.005 \qquad \theta_1 = \theta_2 = 0.70 \pm 0.04 \qquad \nu_x = 0.95 \pm 0.04. \tag{2.17}$$

From now on we will look for further confirmation of our conclusion. In table 4 we show the values of $\theta_{2,N}$ and $\nu_{x,N}$ obtained from the real parts of the energy gaps

Table 4. Values of $\theta_{2,N}$ and $\nu_{x,N}$ obtained from the real parts of the energy gap for the Hamiltonian H at three different assumed positions of the critical point ($\lambda_c = 0.670$, 0.675, 0.680).

	$\theta_{2,N}$			$\nu_{x,N}$		
Intersection $N/(N+1)$	$\lambda_c = 0.670$	$\lambda_c = 0.675$	$\lambda_c = 0.680$	$\lambda_c = 0.670$	$\lambda_c = 0.675$	$\lambda_c = 0.680$
2/3	0.897 560 988	0.910 431 969	0.923 338 943	0.611 315	0.608 798	0.606 395
3/4	0.819 829 899	0.837 534 160	0.855 399 044	0.744 576	0.738 823	0.733 455
4/5	0.778 875 269	0.801 305 801	0.824 099 409	0.817 681	0.807 929	0.799 054
5/6	0.751 384 491	0.778 429 020	0.806 124 688	0.866 159	0.851 717	0.838 916
6/7	0.730 530 453	0.762 078 826	0.794 658 074	0.902 12	0.882 34	0.865 29
7/8	0.713 554 018	0.749 499 664	0.786 952 495	0.930 91	0.905 17	0.883 63
8/9	0.699 106 391	0.739 346 293	0.781 670 308	0.955 24	0.922 96	0.896 74
Estimates	0.63 ± 0.01	0.69 ± 0.01	0.77 ± 0.01	1.06 ± 0.02	1.02 ± 0.01	0.93 ± 0.01

assuming that the critical point is at $\lambda_c = 0.670$, 0.675 and 0.680. The estimates are in agreement with (2.17).

In order to convince ourselves that there is only one phase transition, in figures 3–5 we show the functions $N^{1/2}E(N, \lambda)$, $N^{1/2}F(N, \lambda)$ and $N^{1/2}G(N, \lambda)$ (see (2.8) and (2.9)) which correspond to $\theta_i = \frac{1}{2}$. From figures 3 and 4 one can clearly conclude that there is only one phase transition between a high-temperature modulated phase and a low-temperature ordered phase. Figure 5 is more amusing because the parabola-like curves $N^{1/2}G(N, \lambda)$ intersect twice, say at the values $\lambda_{c,N}^{(1)}$ and $\lambda_{c,N}^{(2)}$, which would suggest two phase transitions. This is however a fluke since the sequences $\lambda_{c,N}^{(1)}$ and $\lambda_{c,N}^{(2)}$ converge to the same value λ_c as can be seen in table 5.

Probably the best estimate for λ_c was obtained considering again the Hamiltonian H (equation (1.12)) with twisted boundary conditions (see von Gehlen and Rittenberg 1984) and computing the energy gap between the ground state with periodic boundary conditions and the first excited state with twisted boundary conditions. This energy

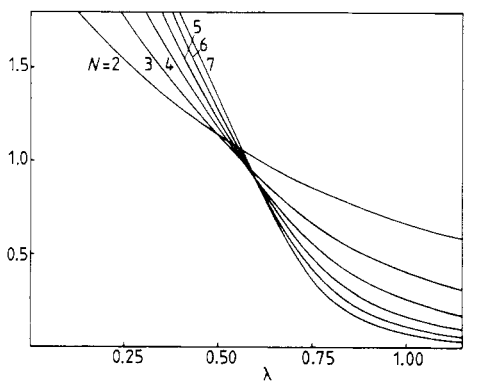

Figure 3. The functions $N^{1/2}E(N, \lambda)$ against λ for $N = 2, \ldots, 7$.

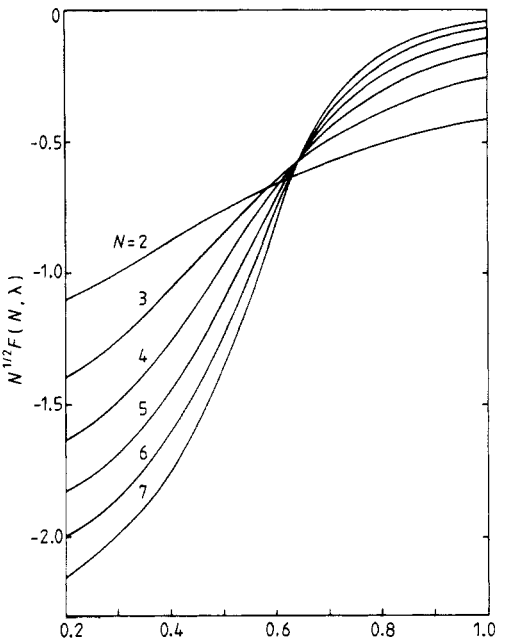

Figure 4. The functions $N^{1/2}F(N,\lambda)$ against λ for $N=2,\ldots,7$.

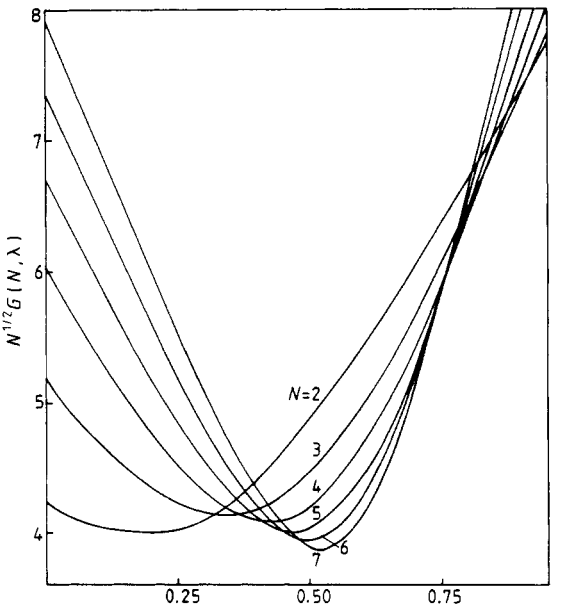

Figure 5. The functions $N^{1/2}G(N,\lambda)$ against λ for $N=2,\ldots,7$.

Table 5. The intersections $\lambda_{c,N}^{(1)}$ and $\lambda_{c,N}^{(2)}$ of the functions $N^{1/2}G(N,\lambda)$ for the Hamiltonian H.

Intersection $N/(N+1)$	$\lambda_{c,N}^{(1)}$	$\lambda_{c,N}^{(2)}$
2/3	0.296 446 913	0.911 862 676
3/4	0.365 659 637	0.838 453 983
4/5	0.412 523 730	0.789 637 502
5/6	0.445 246 45	0.758 634 786
6/7	0.469 103 198	0.737 915 471
7/8	0.487 176 453	0.723 374 084
8/9	0.501 321 577	0.712 761 715
Estimates	0.63 ± 0.03	0.66 ± 0.03

gap vanishes for finite systems and gives good approximants for λ_c. One obtains

$$\lambda_c = 0.667 \pm 0.004 \approx \tfrac{2}{3}. \tag{2.18}$$

We now consider the 'specific heat' $C(N,\lambda)$ (see (2.16)). It is convenient to separate $C(N,\lambda)$ in a smooth background $C_B(\lambda)$ and a 'singular' part $C_S(N,\lambda)$:

$$C(N,\lambda) = C_B(\lambda) + C_S(N,\lambda). \tag{2.19}$$

The functions $C_B(\lambda)$ and $C_S(N,\lambda)$ are shown in figure 6. We have determined the

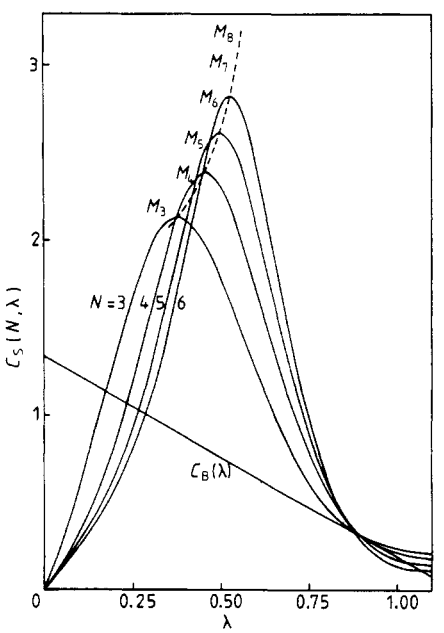

Figure 6. The specific heat $C_S(N,\lambda)$ for $N=3$, 4, 5, 6 and the linear background $C_B(\lambda)$. The positions of the maxima of the curves $C_S(N,\lambda)$ for $N=3,\ldots,8$ are also indicated (the points $M_3,\ldots,M_8$).

ratio α/ν_x (see (2.16)) using $C_S(N, \lambda)$. The estimate is

$$\alpha/\nu_x \approx 0.48 \pm 0.05. \tag{2.20}$$

3. Conclusions

We have taken the x continuum limit of the tranfer matrix corresponding to the asymmetric three-states clock model and have obtained the non-Hermitian Hamiltonians (1.7) for any non-zero asymmetry φ (see (1.2)). We have studied this Hamiltonian and have shown that there is only one phase transition which is *anisotropic* (there are two correlation lengths in the problem). The critical point is

$$\lambda_c = 0.667 \pm 0.004 \tag{3.1}$$

and the critical exponents are

$$\nu_x = 0.95 \pm 0.04 \qquad \nu_\tau = 0.67 \pm 0.04$$
$$\alpha = 0.48 \pm 0.05. \tag{3.2}$$

We stress the fact that the convergence properties in our finite-size scaling study are very good.

Notice that the values (3.2) are compatible with the hyperscaling relation (Hornreich *et al* 1975, Hoeger *et al* 1985)

$$\alpha = 2 - \nu_x - \nu_\tau \tag{3.3}$$

The behaviour of our system is very similar to that observed by Kinzel (1983) in a different model. It is also interesting to point out that the exponents (3.2) are close to those expected for a commensurate-incommensurate phase transition where $\nu_x = 1$, $\nu_\tau = 0.5$ and $\alpha = 0.5$ (see, e.g., Hoeger *et al* 1985).

One can ask what is the relevance of our observation on the phase structure shown in figure 1. This is a very hard question. One possibility is that the line AB in figure 1 represents an anisotropic phase transition and that Duxbury *et al* (1984) have not seen it because the size of their system was too small. Another possibility is that the phase diagram for $g_x \neq g_\tau$ (see (1.2)) is different and that the anisotropic phase transition shows up only for $g_\tau \gg g_x$.

References

Domany E and Schaub B 1984 *Phys. Rev.* B **29** 4095
Duxbury M D, Yeomans J and Beale P D 1984 *J. Phys. A: Math. Gen.* **17** L179
Haldane F D M, Bak P and Bohr T 1983 *Phys. Rev.* B **28** 2743
Hoeger C, von Gehlen G and Rittenberg V 1985 *J. Phys. A: Math. Gen.* **18** 1813
Hornreich R M, Luban M and Shtrikman S 1975 *Phys. Rev. Lett.* **35** 1678
Howes S F 1982 *Phys. Rev.* B **27** 1762
Huse D A 1981 *Phys. Rev.* B **24** 5180
Huse D A and Fisher M E 1982 *Phys. Rev. Lett.* **49** 793
Kinzel W 1983 *Phys. Rev. Lett.* **51** 996
Nightingale M P 1982 *J. Appl. Phys.* **53** 7927
Ostlund S 1981 *Phys. Rev.* B **24** 398
Schulz H J 1983 *Phys. Rev.* B **28** 2746
Selke W and Yeomans J M 1981 *Z. Phys.* B **46** 311
Vanden Broeck J M and Schwartz L W 1979 *SIAM J. Math. Anal.* **10** 659
von Gehlen G and Rittenberg V 1984 *Nucl. Phys.* B **230** 455
—— 1986 to be published